Supplementary Notes

Supplementary Note 1. Number of addressable output modes and the number of degrees of freedom in the disordered metasurface assisted wavefront engineering system

In this supplementary section, we describe the disorder-engineered metasurface and phase-only SLM optical system from the main text in a general mathematical framework to clearly explain why we can address a number of output modes (M) which is larger than the controlled number of independent degrees of freedom (N). We show that the linear operator connecting the input and output optical modes always has a rank $\leq N$ (the number of pixels in the SLM). Therefore, the number of degrees of freedom for the output modes is equal to the rank of the transmission matrix. However, even though we are limited to at most N degrees of freedom for the output modes, it is still possible to have a large number of resolvable focal spots within a field of view.

Any linear optical device can be described by a linear operator T which takes an input function E_i and generates a linear combination of modes E_o, given as

$$E_o = TE_i.$$

In the scenario of disordered media assisted wavefront shaping, T is an $M \times N$ matrix where N is the number of independent modes controlled on the SLM (the number of elements in E_i) and M is the number of addressable focal spots within an area of interest on the other side of the disordered medium (the number of elements in E_o). In general, M is larger than N to take advantage of the disordered medium's ability to access an extended optical space. This transmission matrix is of rank $\leq N$. This means that we cannot exercise complete control over all M target output modes to achieve, for example, a perfect focus with no background. However, as previous work in the field of wavefront shaping has shown[1,2], it is possible to combine the fraction of the N independent input modes (given by the rank of T) that are transmitted through

open channels of the disordered medium to optimize the light intensity delivered into a desired output mode such as a focusing field.

When a disordered medium is used in this way, it is called a "scattering lens." If each resolvable focal spot in the output space was treated as one mode (the total number of which is defined as M according to the space-bandwidth product formalism in the main text), we would seemingly be able to achieve a number of degrees of freedom larger than the rank of our linear system. However, it is not valid to count each resolvable focal spot as an independent mode, because the focal spots created by the scattering lens have correlated, speckle-like backgrounds. Although the number of resolvable focal spots is not equivalent to the number of degrees of freedom, it is an important and useful parameter in many applications. In our focus-scanning scattering lens microscope, since the intensity of an achieved focal spot is significantly higher ($>10^4$) than the background intensity, we can count the addressed focal spots as resolvable focal spots.

Supplementary Note 2. Conventional measurement of the transmission matrix using *O(P)* measurements

In previous reports, measurements of the transmission matrix have been performed in one of two ways. The first method can be implemented by displaying N orthogonal patterns on the SLM and recording the output field for each pattern[3,4]. This approach can be understood as measuring the transmission matrix one column at a time, where each column corresponds to one SLM pattern, and each element in the column represents the output field contribution at a unique focal point on the projection plane. To focus to a given point on the projection plane, the pattern displayed on the SLM is selected as a linear combination of the SLM patterns such that the output field constructively interferes at the desired focal point. In the context of phase-only modulation, this

means that the phase of each field vector, controlled by their respective pixels on the SLM, is aligned so as to maximize the sum over all the field vectors at that location. In order to enable focusing at all M focal spots, the output field for each SLM pattern must be measured at each of the M focal spot locations.

An alternate way to measure the transmission matrix is using optical phase conjugation[5]. This scheme is typically implemented by creating a calibration light focus from an external lens positioned at the desired focus location and recording the optical field transmitted in the reverse direction through the disordered medium toward the SLM. Then this procedure is repeated by scanning the focus to all M desired focal spots on the output plane. Mathematically, this approach can be interpreted as measuring the transmission matrix one row at a time, where the elements in each row describe the phase and amplitude relationship between a pixel on the SLM and the desired focal point.

While both of these approaches provide a way to characterize the transmission matrix of a disordered medium, they each suffer from practical limitations that prevent them from being practically useful for achieving control over large transmission matrices ($P > 10^{12}$). These stem from the sheer number of measurements and time required to characterize the transmission matrix. The first method is infeasible for large M due to the lack of commercially available camera sensors with the required number of pixels. Thus far, to the best of our knowledge, the largest reported transmission matrix measured using this method contained $P = 10^8$ elements. While the second method is not limited by the availability of the requisite technology, it requires mechanically scanning the focus to each spot. Assuming the relevant measurement technology existed for both cases, with a measurement speed of 10^8 measurements (i.e. transmission matrix elements) per second (equivalent to 5 megapixels at 100 frames per second), the measurement

for all $P = 10^{13}$ elements in our demonstrated transmission matrix would require a measurement time of over 24 hours. To make matters worse, conventional disordered media used with wavefront engineering such as white paint made of TiO_2 or ZnO nanoparticles have a stability of only several hours [1,6,7], so the measured transmission matrix would be invalid by the time the measurement was complete.

Supplementary Figures

Supplementary Figure 1

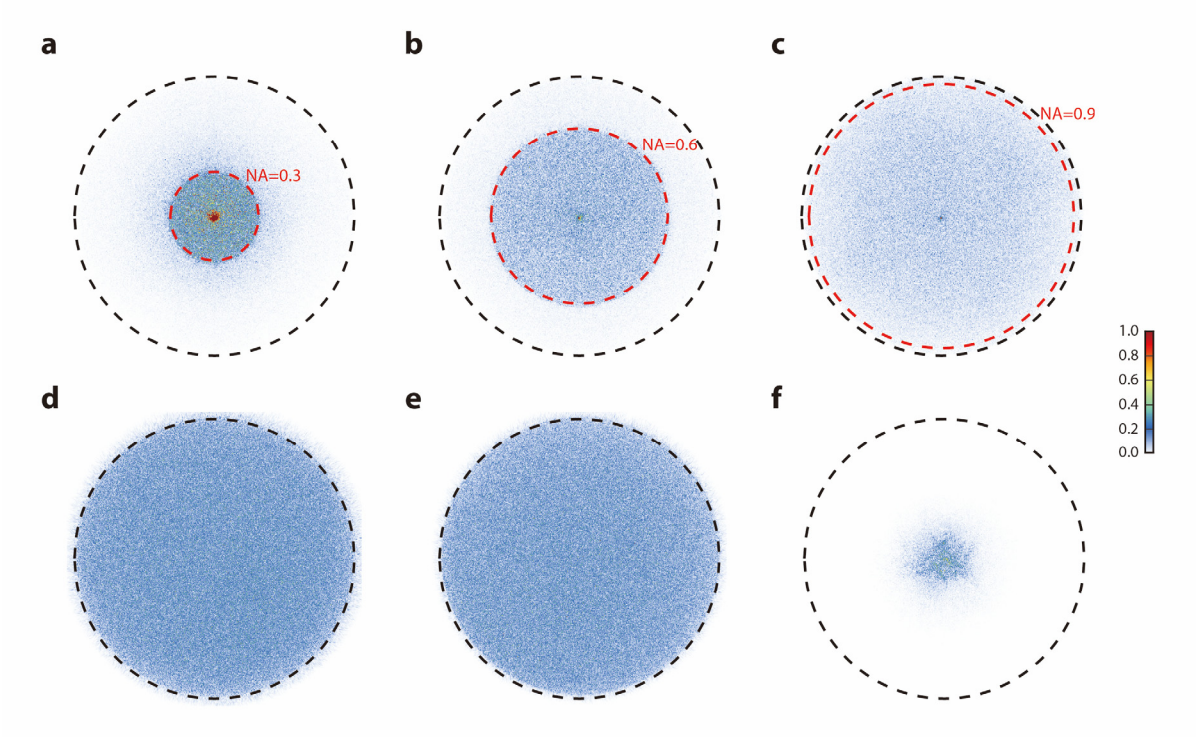

Supplementary Figure 1. Measured angular scattering profiles of disordered metasurfaces as well as those of conventional disordered media. A collimated laser beam illuminated the scattering media and a 4-*f* system imaged the back focal plane of an objective lens (NA = 0.95) to a camera. (**a** to **c**) Angular scattering profiles of disordered metasurfaces with different designs, normalized to strongest scattered field component. The disordered metasurfaces were specifically designed such that they scatter the incident light to certain angular ranges of (**a**) NA = 0.3, (**b**) 0.6, (**c**) 0.9, which are denoted with red dotted lines. See also Fig. 2c in the main text for the scattering profiles of the disordered metasurface used in the experiment. (**d** to **f**) Angular scattering profiles of conventional scattering media. (**d**) The 20-μm-thick white paint (made of TiO_2 nanoparticles) and (**e**) opal glass diffuser (10DIFF-VIS, Newport) show isotropic scattering over the wide angular ranges, while (**f**) the ground glass diffuser (DG10-120, Thorlabs) has a

very limited angular range for scattering. The black dotted lines correspond to the cutoff frequencies of the objective lens (NA = 0.95), which is the limit in our measurement setup.

Supplementary Figure 2

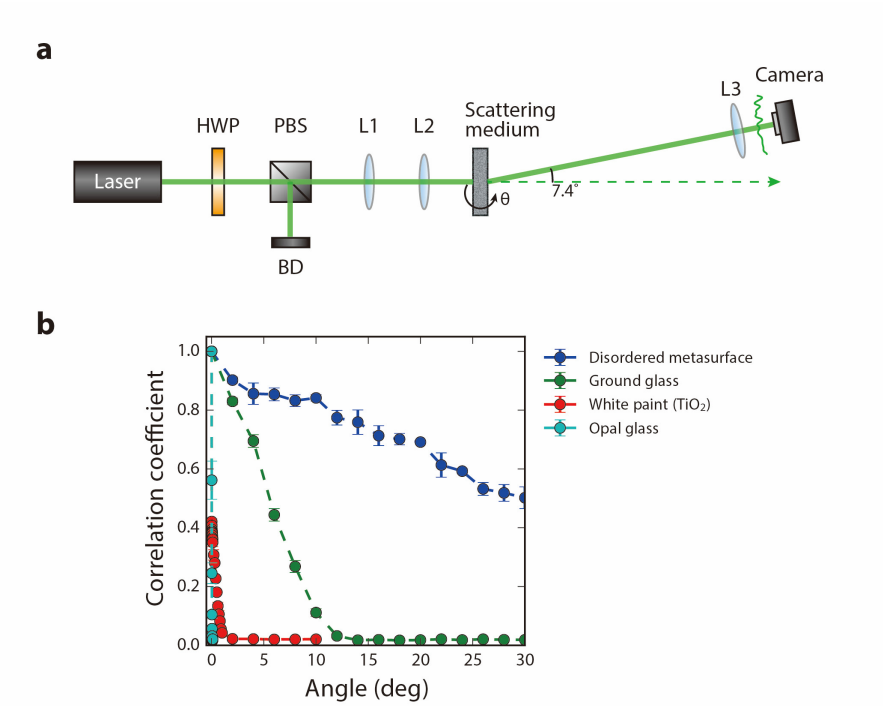

Supplementary Figure 2. Optical memory effect measurement. (**a**) Schematic of the optical setup to measure the angular correlation range of different scattering media. The output of a long coherence length, 532-nm, continuous-wave laser was attenuated by a variable attenuator composed of a half-wave plate (HWP) and a polarizing beam splitter (PBS) where the unwanted power was sent into a beam dump (BD). After it was expanded to a beam diameter of 8 mm by lenses L1 and L2, the laser beam illuminated the scattering medium to be tested, and the speckle pattern was detected by a camera. The camera and a camera lens L3 were positioned 7.4 degrees from the optical axis, to avoid collecting any undiffracted light. The series of speckle patterns were recorded as we rotated the scattering medium, and we computed the correlation coefficient between the first frame and each of the ensuing frames. (**b**) The measured memory effect ranges for the disordered metasurface, ground glass (DG10-120, Thorlabs), opal glass (10DIFF-VIS,

Newport), and 20-μm-thick white paint (made of TiO_2 nanoparticles). See also Fig. 2e in the main text. Error bars indicate the standard deviation of three measurements.

Supplementary Figure 3

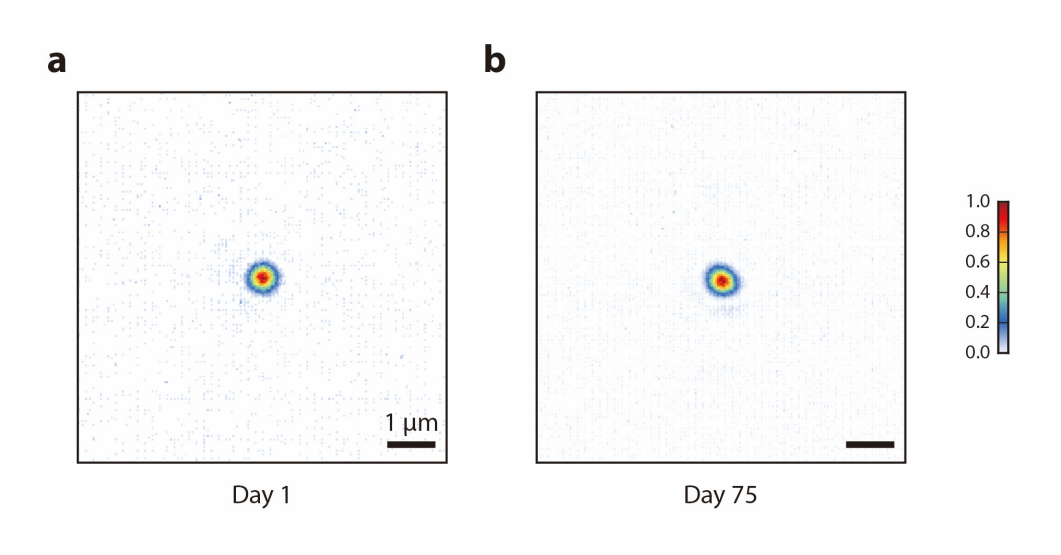

Supplementary Figure 3. Extraordinary stability of a disordered metasurface. Over a period of 75 days, a high quality optical focus was obtained from the same metasurface without observable efficiency loss by small system alignments to compensate for mechanical drift. (**a**) Reconstructed focus on the 1st day. The measured contrast was 19,800. (**b**) Reconstructed focus on the 75th day. The measured contrast was 21,500. Scale bar: 1 µm.

Supplementary Figure 4

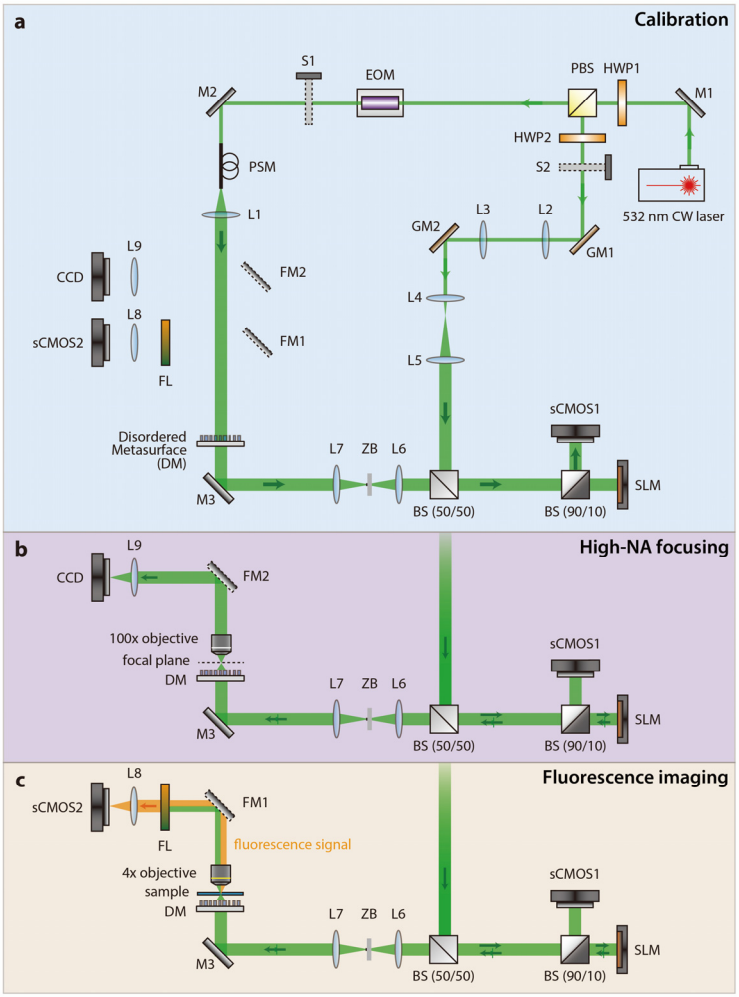

Supplementary Figure 4. Experimental setup. See Methods for detailed procedures for different experiments. (**a**) Phase-shifting holography setup used for calibrating the alignment for the disordered metasurface and the SLM. Zeroth-order block between L7 and L6 was used to block an undiffracted light from the disordered metasurface, which was experimentally measured to be 1.5% with respect to the incident intensity. (**b**) Custom-built microscope setup used for characterizing high-NA focusing over a wide-FOV. (**c**) Focus-scanning fluorescence imaging setup. M: mirror, L: lens, HWP: half-wave plate, PBS: polarizing beam splitter, S: shutter, EOM: electro-optic modulator, GM: galvanometric mirror, BS: beam splitter, sCMOS: scientific CMOS camera, CCD: CCD camera, SLM: spatial light modulator, ZB: zeroth-order block, DM:

disordered metasurface, FM: flip mirror, PSM: polarization-maintaining single-mode fiber, FL: fluorescence filter.

Supplementary Figure 5

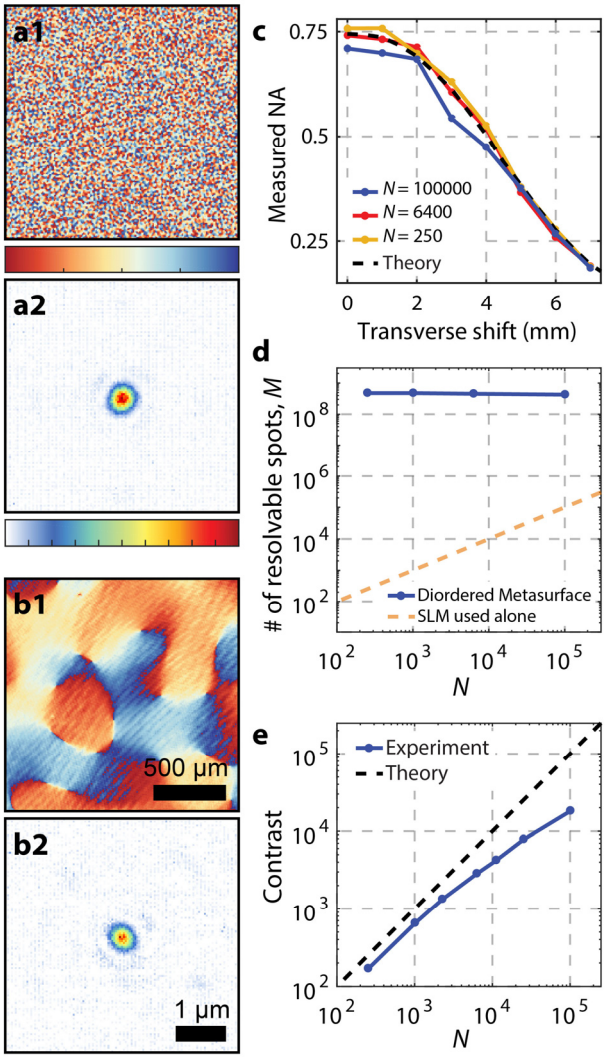

Supplementary Figure 5. Demonstration of ultra-high number of resolvable spots *M* (~4.5×10^8) even with a handful of physically controlled degrees of freedom (~2.5×10^2) as inputs. (**a1-2, b1-2**) Cropped phase images displayed on the SLM (**a1**, **b1**) as well as the corresponding 2D intensity profiles (**a2**, **b2**) of the foci reconstructed at z' = 3.8 mm on axis (NA = 0.75). The controlled number of input optical modes displayed SLM was (**a1**) 1.0×10^5 and (**b1**) 2.5×10^2, respectively. Scale bars for the phase images and the 2D intensity profiles are 500 μm and 1 μm, respectively. (**c**) Measured NA of the foci created along *x*-axis. The measured NA shows good agreement with theory, regardless of the number of input modes controlled on the

SLM. (**d**) Measured number of resolvable spots M as a function of the number of optical modes N controlled on the SLM. (**e**) Dependence of contrast factor η on the number of optical modes controlled on the SLM.

Supplementary Figure 6

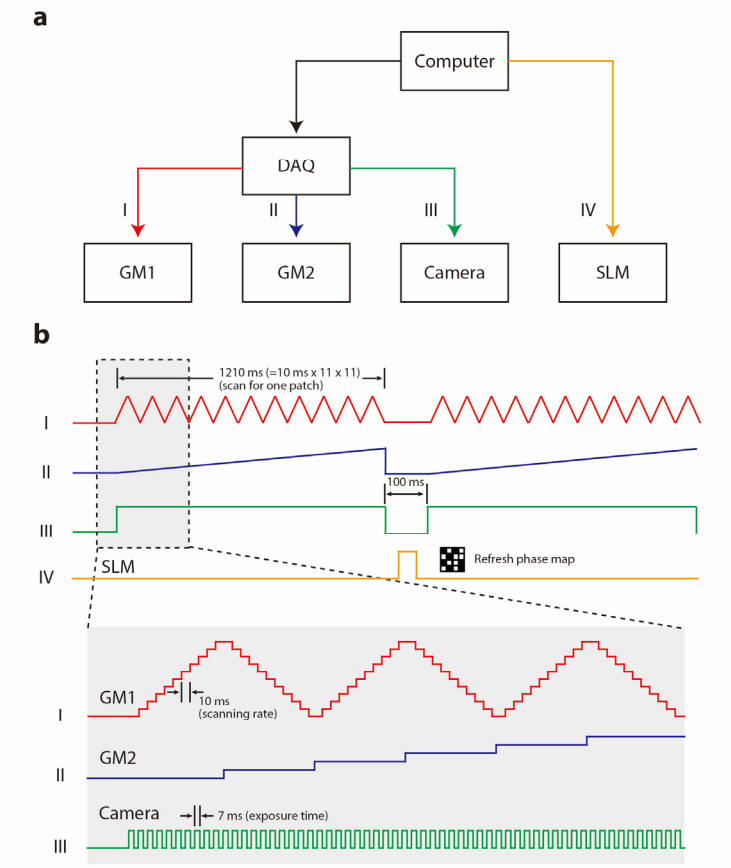

Supplementary Figure 6. Electrical signal flow diagram for scanning fluorescence imaging. (**a**) The system control diagram. (**b**) A data acquisition card (DAQ) outputted voltage stepping signals to a pair of galvanometric mirrors (GM1 and GM2) to perform bi-directional raster scanning with a pixel dwell time of 10 ms. At the same time, the DAQ outputted a synchronized trigger signal with a 7 ms duration (corresponding to the exposure time) to a camera for detecting fluorescent signals. After one patch of 11×11 spots were scanned by the galvanometric mirrors, the galvanometric mirrors returned to the original position. During a 100 ms period, the phase map for correcting coma aberration was updated on a spatial light modulator (SLM). Then, the raster scanning by the galvanometric mirrors was resumed again to constitute another patch.

Supplementary Figure 7

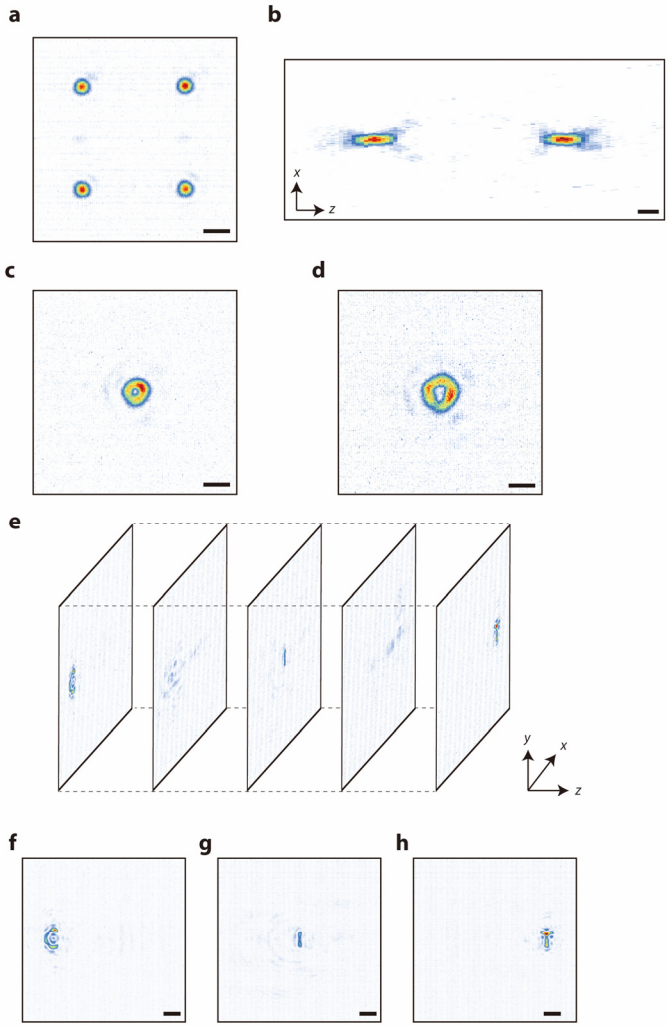

Supplementary Figure 7. Demonstration of arbitrary complex wavefront modulation with a disordered metasurface. (**a, b**) Simultaneous generation of multiple foci. Scale bars: 1 μm. (a) Four foci on a 4 μm pitch grid were reconstructed simultaneously along the lateral axes. (b) Two foci separated by 10 μm were reconstructed simultaneously along the optical axis. (**c, d**) Optical vortex focusing with topology charges of (**c**) m=1 and (**d**) m=2. Scale bars: 1 μm. (**e** to **h**) 3D display using letters of 'C', 'I', and 'T' placed at (**f**) z = -10 μm, (**g**) 0 μm, and (**h**) 10 μm. Scale bars: 2 μm.

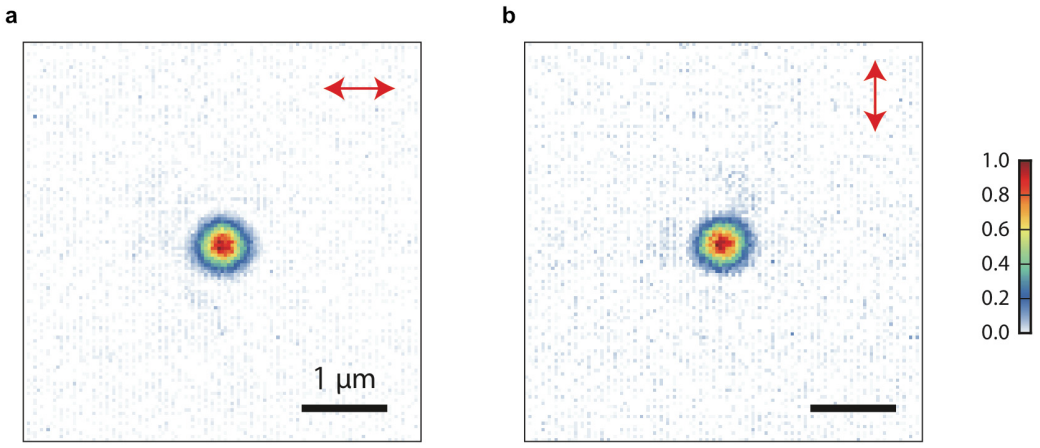

Supplementary Figure 8. Demonstration of polarization insensitivity of current disordered metasurface design. Due to the symmetry of the lateral size of the nano-posts, the current disordered metasurface design is insensitive to the incident polarization state. Foci with (**a**) horizontal and (**b**) vertical linear polarizations.

Supplementary References

1. Vellekoop, I. M. & Mosk, A. P. Focusing coherent light through opaque strongly scattering media. *Opt. Lett.* **32,** 2309–2311 (2007).
2. Vellekoop, I. M., Lagendijk, A. & Mosk, A. P. Exploiting disorder for perfect focusing. *Nat. Photonics* **4,** 320–322 (2010).
3. Popoff, S. M. *et al.* Measuring the transmission matrix in optics: An approach to the study and control of light propagation in disordered media. *Phys. Rev. Lett.* **104,** 1–4 (2010).
4. Choi, Y. *et al.* Overcoming the diffraction limit using multiple light scattering in a highly disordered medium. *Phys. Rev. Lett.* **107,** 1–4 (2011).
5. Yaqoob, Z., Psaltis, D., Feld, M. S. & Yang, C. Optical phase conjugation for turbidity suppression in biological samples. *Nat. Photonics* **2,** 110–115 (2008).
6. Choi, Y., Yoon, C., Kim, M., Choi, W. & Choi, W. Optical imaging with the use of a scattering lens. *IEEE J. Sel. Top. Quantum Electron.* **20,** 61–73 (2014).
7. Yoon, J., Lee, K., Park, J. & Park, Y. Measuring optical transmission matrices by wavefront shaping. *Opt. Express* **23,** 10158–10167 (2015).